

Electronic Supplementary Information.

Solvent-free phenyl-C61-butyric acid methyl ester (PCBM) from clathrates: insights for organic photovoltaics from crystal structures and molecular dynamics.

Mosè Casalegno^a, Stefano Zanardi^b, Francesco Frigerio^b, Riccardo Po^c, Chiara Carbonera^c, Gianluigi Marra^c, Tommaso Nicolini^a, Guido Raos^a, Stefano Valdo Meille^{a*}

^a Dipartimento di Chimica, Materiali e Ingegneria Chimica “G. Natta”, Politecnico di Milano, via Mancinelli 7, I-20131 Milano (MI), Italy.

^b ENI Refining and Marketing, via Maritano 26, I-20097 San Donato Milanese (MI), Italy.

^c Research Centre for Non-Conventional Energies, ENI Istituto Donegani, Via Fauser 4, I-28100 Novara (NO), Italy.

Experimental

Materials: The PCBM sample used for all measurements in the present study was purchased from Aldrich (purity > 99%, cat. 668430). The original sample was highly crystalline and displayed a powder diffraction pattern identical to the one reported by Piersimoni et al. for a sample purchased from Solenne. The experimental density of the as-purchased sample was $1.613 \pm 0.006 \text{ Mg/m}^3$ and was determined by floatation in an aqueous NaI solution. Cocrystals with *ortho*-dichlorobenzene were easily obtained by recrystallization from the same solvent by slow evaporation at room temperature. The *ortho*-dichlorobenzene cocrystals retransformed into the commercial crystalline modification by annealing at 90°C-100°C, typically for 48 hours.

Thermal characterization

I) DSC:

Thermal characterization was performed with a Mettler Toledo DSC 822 instrument. Scans were carried out at 10°C/min under 50 ml/min N₂ flow, from 30 to 310°C (**Figure S1**)

The thermal of n-PCBM and n'-PCBM is in essence identical and corresponds to already published data of commercial products. The first heating cycles often present a weak endotherm around 110°C suggesting that impurities of the *oDCB*-PCBM polymorph (see below) might be present.

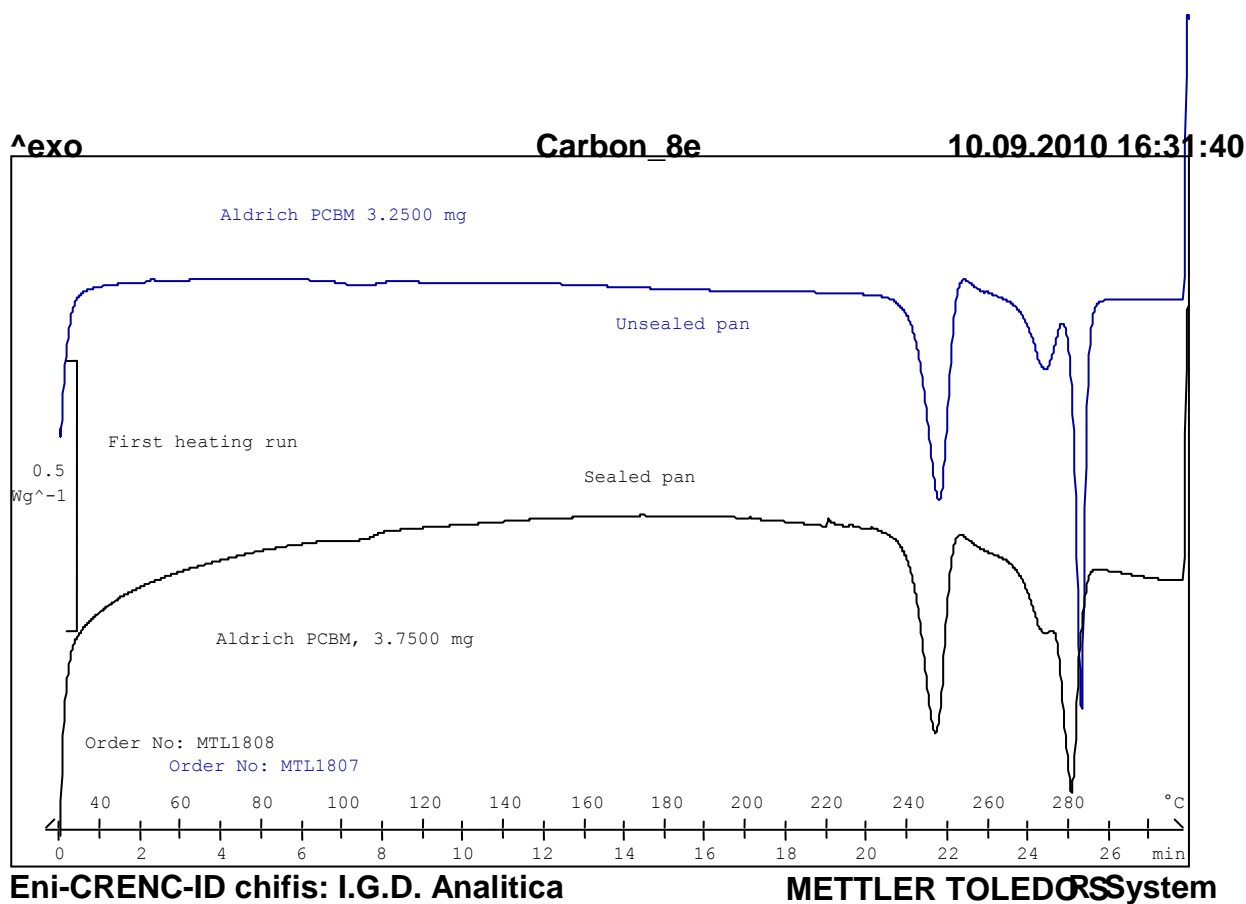


Figure S1

The thermal characterization of native oDCB-PCBM is shown below. All measurements have been performed using Al unsealed pans, under an N₂ flux of 50 ml/min. The two Figures represent the first (**Figure S2**), and the second and third (**Figure S3**, continuous and dashed lines respectively) heating scans. The temperature ranges from 30 to 310°C in the first heating and from -50 to 310°C for the other two scans. Notice that after solvent evolution, at the heating rate of 10°C/min, the sample does not manage to transform into the *n*-PCBM phase but plausibly eventually recrystallizes into a “high temperature” phase.

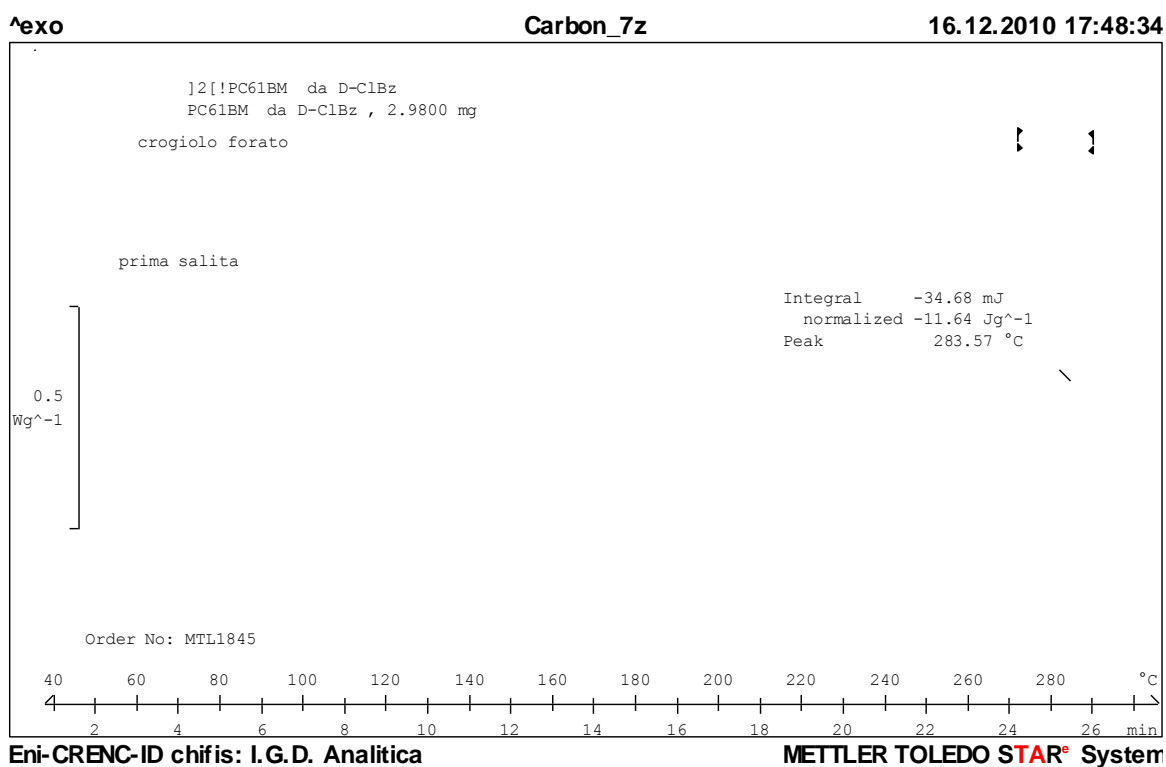


Figure S2

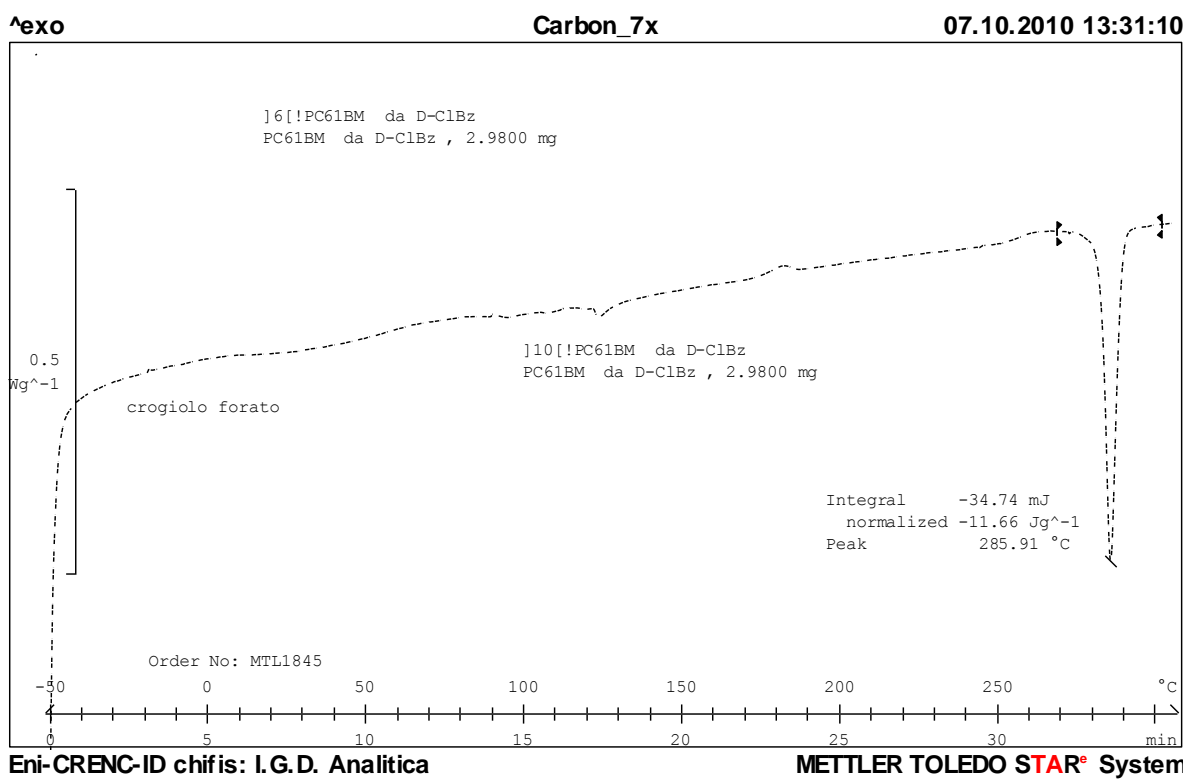


Figure S3

II) TGA:

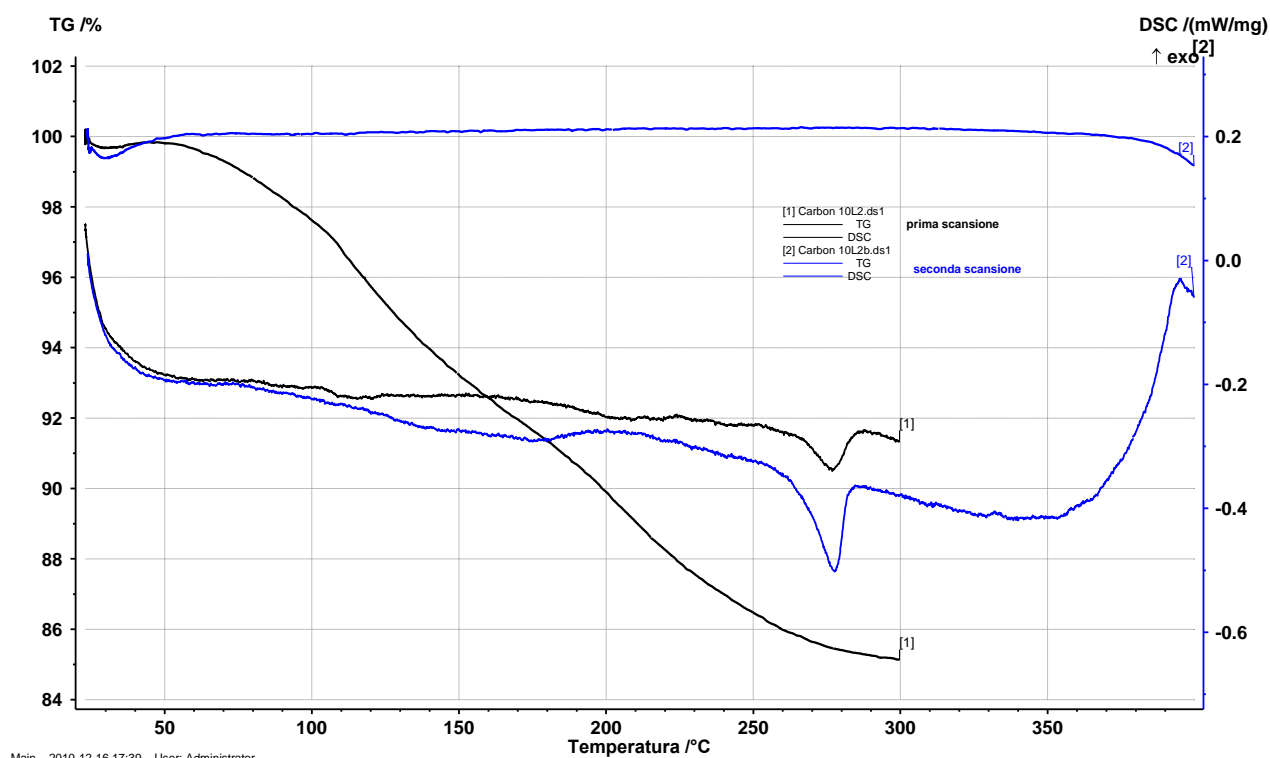


Figure S4

Thermogravimetric analyses were performed with a TG-DSC STA 449 *F1 Jupiter*[®] (NETZSCH). **Figure S4** above refers to the following experiment: a 7.03 mg oDCB-PCBM sample was first heated in a HP crucible in the Mettler Toledo DSC 822 instrument. Then, 3.56 mg of the material were extracted and analysed thermogravimetrically with the following conditions: 10°C/min; N₂ flux 50ml/min; temperature range 25°-300°C. Then, the rest of the original 7 mg sample underwent a second heating in Mettler instrument and at the end of the thermal treatment (3.28 mg) to Jupiter thermogravimetric analysis was performed with the following parameters: 10°C/min; N₂ 50ml/min; in the 25°-400°C temperature interval.

Scanning Electron Microscopy

Morphological characterization was performed by Field Emission Scanning Electron Microscopy (FESEM) using a JEOL 7600F high-resolution microscope with field emission source for hot cathode Schottky type, secondary electron detector "semi-in-lens"; the acceleration of the electron varying from 0.1 to 30 kV and the maximum resolution of 1.0 nm at 15 kV. In Figure S5 three typical micrographs of the three samples discussed in the paper are shown.

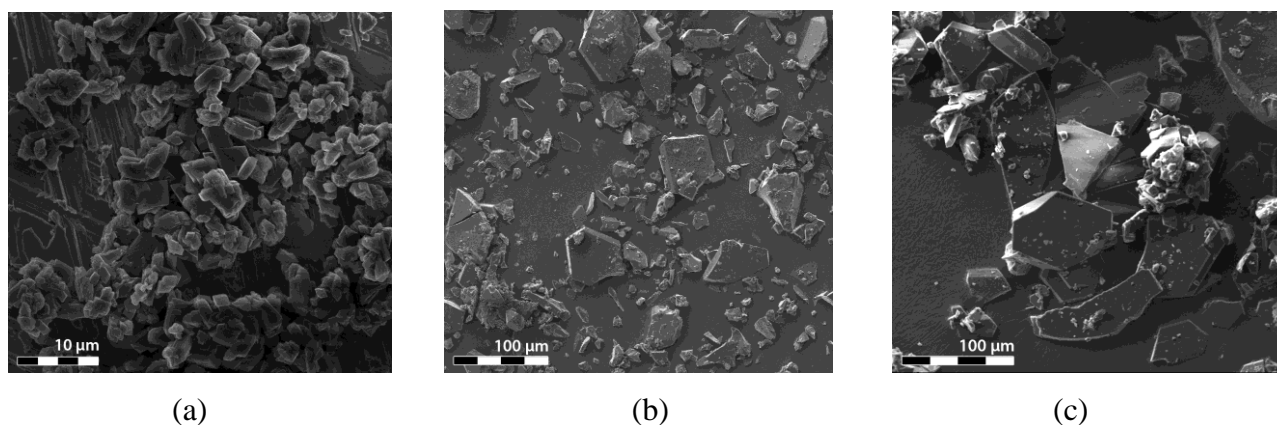


Figure S5

SEM micrographs of (a) as-purchased *n*-PCBM and (b) *o*DCB-PCBM crystal obtained by slow crystallization from *o*DCB, (c) *n*-PCBM obtained by vacuum treatment at temperatures up to 90°C of *o*DCB-PCBM single crystals shown in b). It must be stressed that shape retention of the morphological entities of *n*-PCBM in c), obtained removing *o*DCB, does not mean that the single crystal nature is preserved. In fact it is not (see Fig. S9 below) and the morphological units in c) are aggregates of microcrystals. Rietveld refinement procedures (see below) indicate significant preferred orientation: the original (1 0 -1) main faces of the *o*DCB-PCBM single crystalline platelets tend to become preferentially parallel to (0 1 1) planes of *n*-PCBM microcrystals in the aggregates shown in c).

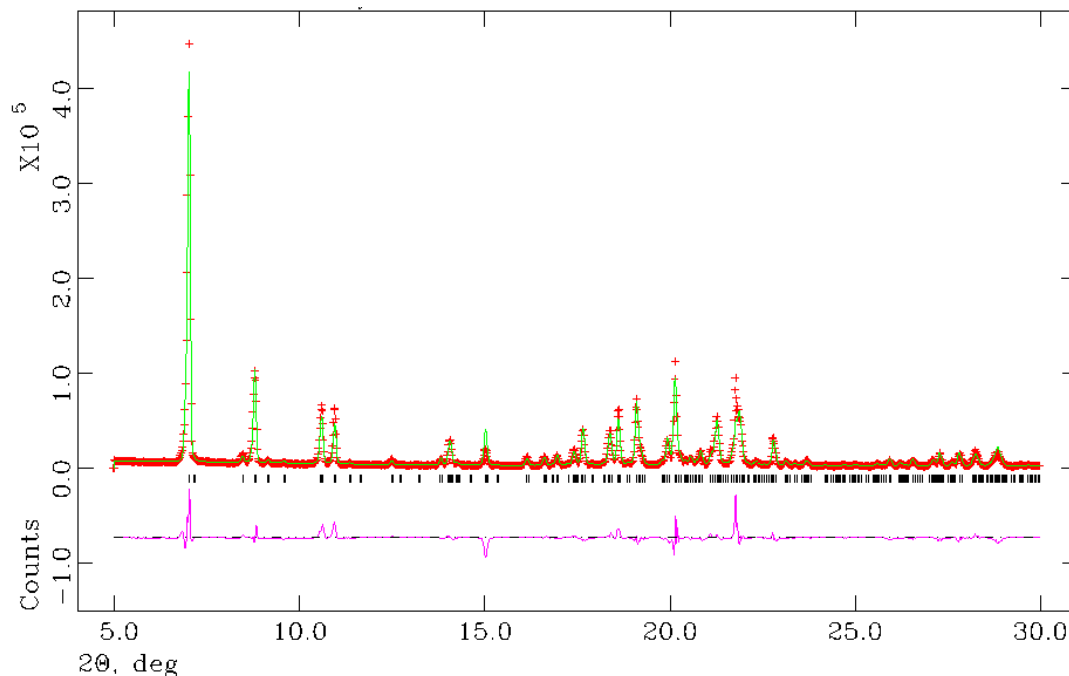
X-ray diffraction and morphological analysis:

I) Room temperature *o*DCB-PCBM structure

Powder X-ray diffraction data were recorded on a Panalytical X'Pert laboratory diffractometer equipped with a PW3050/60 θ/θ goniometer and an X'Celerator RTMs detector using Ni-filtered Cu- $K\alpha$ radiation. Data collection procedures similar to those detailed for *n*-PCBM in the enclosed *n*-PCBM.CIF file were used. The final Rietveld plot for the *o*DCB-PCBM structure at room temperature is reported in **Figure S6**. The refinement was carried out using the software GSAS [RS1, RS2] starting from the structural data in reference RS3. During the refinement the adopting the original $P2_1/n$ space group the lattice parameters expanded from the original values of $a = 13.7565(9)$, $b = 16.634(1)$, $c = 19.077(1)$ Å, $\beta = 105.289(1)^\circ$, $V = 4210.8(4)$ Å³ to $a = 13.954(1)$, $b = 16.709(1)$, $c = 19.223(1)$ Å, $\beta = 105.851(4)^\circ$, $V = 4311.3(4)$ Å³, implying a 2.3% density decrease. To obtain a reasonable fit it was necessary to take into account a clear preferred orientation effect (March-Dollase approach, 0.618 ratio along the $\langle 1\ 0\ -1 \rangle$ direction) fully consistent with the platelet morphology of the sample. Coordinates were kept fixed during the least square procedure, whereas the atomic displacement parameters were subjected to a constrained

refinement and converged to relatively high but reasonable values. The final discrepancy factors ($R = 0.107$; $wR = 0.149$), considering preferred orientation effects and the overall quality of the data and of the refinement confirm that the room temperature *o*DCB-PCBM data, except for the lattice expansion and preferred orientation correspond to the same structure as already reported in RS3.

Figure S6



Single crystals of *o*DCB-PCBM:

Single crystals of *o*DCB-PCBM (**Figure S7**) were obtained by slow evaporation from an *o*-dichlorobenzene solution and washed to eliminate germination. The unit cell was determined on a Bruker P4 diffractometer, using graphite monochromated Cu- $K\alpha$ radiation, at 298K.

Determined lattice parameters.:

Single crystal:

$$a = 13.941(2) \text{ \AA}$$

$$b = 16.671(3) \text{ \AA}$$

$$c = 19.210(3) \text{ \AA}$$

$$\beta = 105.90(1)^\circ$$

$$V = 4293.6(9) \text{ \AA}^3$$

They are in good agreement with the results of the powder refinement.

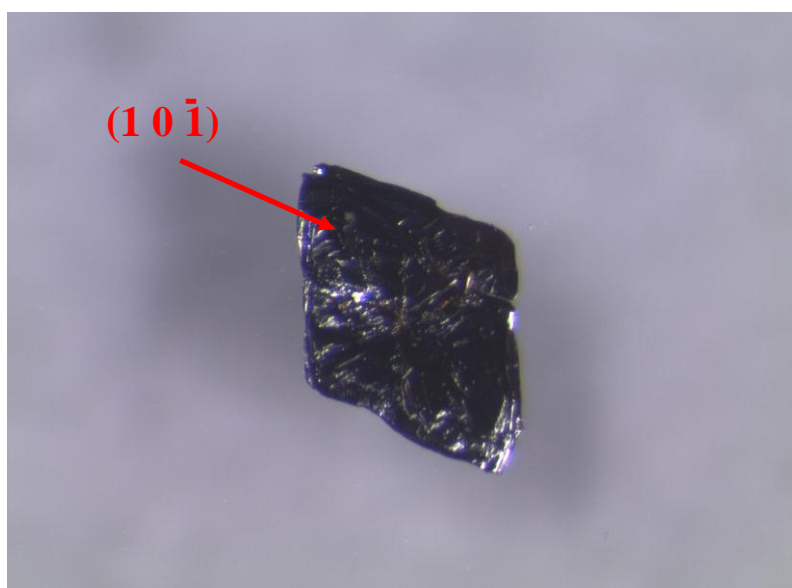


Figure S7

(Crystal dimensions ca. 0.3 mm x 0.3 mm x 0.04 mm)

Face indexing procedure allowed to identify unequivocally the lamellar plane, i.e. the largest face of the crystal as (1 0 -1). Because of the thinness of the platelets the indexing of the lateral faces was less straightforward and some of lateral faces which were identified on different single crystals examined are: (0 1 0), (-1 1 2), (2 1 0). By annealing, single crystals of *o*DCB-PCBM at 90° C for 48 h under vacuum turned into polycrystalline specimen. An image of a crystal after the thermal treatment and its polycrystalline diffraction pattern, corresponding to the *n*'-PCBM pattern, are respectively reported in **Figures S8** and **S9**.

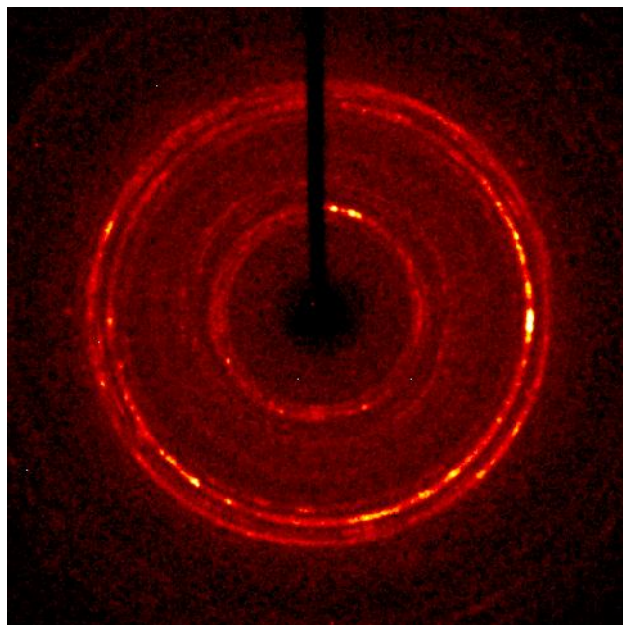


Figure S8

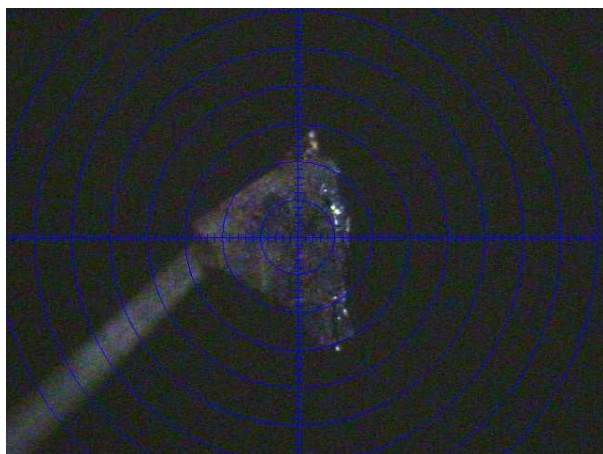


Figure S9

Room temperature *n*-PCBM structure (Aldrich sample, purity > 99%, cat. 668430)

Details of the data collection, of the structure solution and of the structural refinement have been deposited with the Cambridge Crystallographic Data Centre as supplementary publication no. CCDC-907694. The resolution was accomplished starting from the internal coordinates of PCBM in the *o*DCB-PCBM crystal structure (ref. RS3) and allowing for variations, in a thermal annealing search, initially of four side chain torsion angles (Φ_2 , Φ_3 , Φ_5 and Φ_6 , see Figure 2 of the paper and Table S1) selected considering also the different conformations shown by PCBM in the two independent molecules in *MCB*-PCBM(ref. RS3). The space group is $P2_1/n$ and refined lattice parameters values are $a = 13.4951(5)$, $b = 15.1572(4)$, $c = 19.0964(7)$ Å, $\beta = 107.142(2)^\circ$. In Table S1 refined torsion angle values for *n*-PCBM (e.s.d. in parentheses) and corresponding values for *o*DCB-PCBM and for the two independent molecules of *MCB*-PCBM crystals are reported. One short interfullerene C...C contacts 2.87 Å, other above 3.16 Å.

Structure	Φ_1 C72-O1-C71-C70	Φ_2 O1-C71-C70-C69	Φ_3 C71-C70-C69-C68	Φ_4 C70-C69-C68-C61	Φ_5 C69-C68-C61-C59	Φ_6 C63-C62-C61-C59
<i>n</i> -PCBM	-178 (2)	123.5 (9)	-44.7(9)	175.7(3)	-150.8(6)	-56.3(4)
<i>o</i> DCB-PCBM ^{a)}	178.1	143.8	-60.96	174.8	-138.5	-49.18
MCB-PCBM (1) ^{b)}	176.2	73.3	-178.1	175.0	153.4	-39.4
MCB-PCBM (2) ^{b)}	174.3	-70.7	76.6	-173.6	68.65	-59.3

Table S1: Refined torsion angle values for *n*-PCBM (e.s.d. in parentheses) and corresponding values reported for *o*DCB-PCBM and for the two independent molecules of MCB-PCBM crystals

II) Analysis of *n*-PCBM sample obtained annealing *o*DCB-PCBM for 48h at 90°C

Powder X-ray diffraction data (see Figure S10 for the lower angle portion of the pattern) were recorded also in this case on a Panalytical X'Pert laboratory diffractometer, equipped however with a secondary graphite monochromator and a scintillation counter. The data collection range was 5.00-89.98° (2θ) and a step scan mode with a 0.02° step and a counting time of 20 s was used with a Cu sealed tube source. Refinement procedures using TOPAS-Academic [RS4], similar to those detailed for *n*-PCBM in the enclosed *n*-PCBM.CIF file were adopted. To optimize the fit it was necessary to take into account substantial preferred orientation effects, and best results are obtained with a uniaxial March-Dollase approach and a 0.66 parameter along the $\langle 0\ 1\ 1 \rangle$ direction, very similar numerically to the value found in the originating *o*DCB-PCBM sample. The final discrepancy factors were of the order of $R_1 = 0.11$; $wR = 0.15$ using a refinement procedure closely comparable to that detailed in the rev-*n*-PCBM.CIF file: results are visually indistinguishable from those in Fig. 1 of the paper but never quite as satisfactory as with the *n*-PCBM data set, probably due to the sample morphology and to the fact that preferred orientation is not taken into account fully satisfactorily.

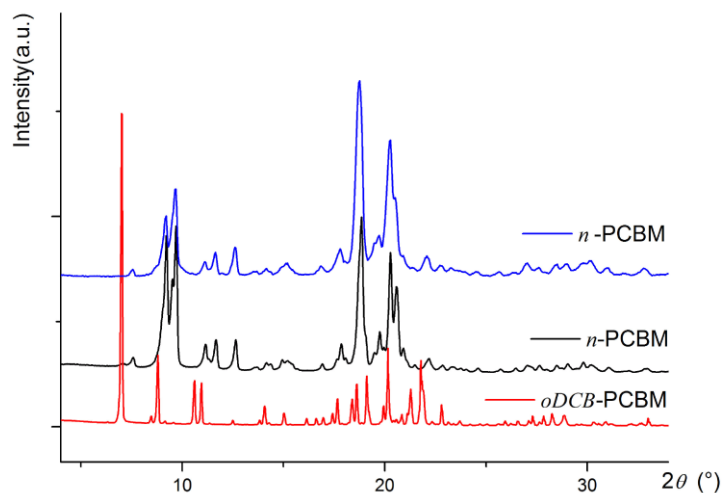


Figure S10

Powder X-ray diffraction patterns of the as-purchased “native” *n*-PCBM sample (black), of *o*DCB-PCBM (red, at the bottom) obtained by slow recrystallization of *n*-PCBM from *o*-dichlorobenzene, and of the *n*-PCBM sample (blue, at the top) obtained annealing at 100°C under vacuum *o*DCB-PCBM.

Molecular Dynamics:

The atomistic force field we used in MD simulations was developed from the OPLS-AA model according to our previous work [RS5]. The electrostatic interactions were calculated using the Particle-Mesh-Ewald method [RS6], with a real space cutoff of 1.2 nm. The same cutoff was used also for the truncation of the LJ interactions. All calculations were performed with the GROMACS4 package [RS7], using the Nose-Hoover thermostat for temperature control (coupling constant $\tau_T=0.1$ ps) and Parrinello-Rahman method for pressure control (coupling constant $\tau_P=1.0$ ps).[RS8] The compressibility value was set equal to that of C₆₀ in the solid phase, 7×10^{-6} bar⁻¹ [RS9]. A time step of 1 fs was used in all simulations.

To test the stability of the n-PCBM structure, two 50 ns runs were performed at 300 and 400 K, NPT simulations carried out with a 2x2x2 supercell, relaxing the symmetry to *P1* at a constant pressure of 1 bar. In the 300K (average over 500 frames) run the monoclinic symmetry was in essence preserved yielding the following average lattice parameters: $a = 13.441$ (-0.40 %), $b = 15.029$ (-0.85%), $c = 19.614$ (+2.71%) Å, $\alpha = 90.09^\circ$, $\beta = 108.94^\circ$ (from 107.142°); $\gamma = 90.15^\circ$.

The data shown in Figure 3 of the paper were obtained according to the following procedure. For each of the investigated structures (oDCB-PCBM, CB-PCBM, and n-PCBM) a preliminary equilibration run (50 ns) was performed at constant pressure (1 bar) and temperature (300 K). Then, a production run (50 ns) was carried out at the same temperature and at constant volume. The radial distribution functions and coordination numbers were averaged over 5000 configurations.

[RS1] A.C. Larson, R.B. Von Dreele, "General Structure Analysis System (GSAS), Los Alamos National Laboratory Report LAUR-86-748, 2004.

[RS2] B.H. Toby, EXPGUI, a graphical user interface for GSAS, J. Appl. Crystallogr. 2001, 34, 210.

[RS3] M. T. Rispens, A. Meetsma, R. Rittberger, C. J. Brabec, N. S. Sariciftci and J. C. Hummelen, "Influence of the solvent on the crystal structure of PCBM and the efficiency of MDMO-PPV:PCBM 'plastic' solar cells" Chem. Commun., 2003, 2116–2118.

[RS4] Coelho, A. A. TOPAS-Academic V4.1, 2008.

[RS5] F. Frigerio, M. Casalegno, C. Carbonera, T. Nicolini, S. V. Meille, G. Raos. "Molecular dynamics simulations of the solvent- and thermal history-dependent structure of the PCBM fullerene derivative" J. Mater. Chem., 2012, 22, 5434.

[RS6] T. Darden, D. York, and L. Pedersen, "Particle mesh Ewald: An Nlog(N) method for Ewald

sums in large systems”, *J. Chem. Phys.* 1993, 98, 10089–10092.

[RS7] B. Hess, K. Kutzner, D. van der Spoel, E. Lindahl, “GROMACS 4: Algorithms for Highly Efficient, Load-Balanced, and Scalable Molecular Simulation” *J. Chem. Theory Comput.* 2008, 4, 435-447.

[RS8] M. Tuckerman, “Statistical Mechanics: Theory and Molecular Simulation”, Oxford University Press, Oxford and New York, 2010.

[RS9] J. E. Fisher, P. A. Heiney, A. R. McGhie, W. J. Romanow, A. M. Denenstein, J. P. McCauley, Jr., and A. B. Smith III “Compressibility of Solid C₆₀” *Science* 1991, **252**, 1288-1290.